A novel erythroid anion exchange variant (Gly796Arg) of hereditary stomatocytosis associated with dyserythropoiesis

Achille Iolascon,[1] Luigia De Falco,[1] Franck Borgese,[2] Maria Rosaria Esposito,[1] Rosa Anna Avvisati,[1] Pietro Izzo,[3] Carmelo Piscopo,[1] Helene Guizouarn,[2] Andrea Biondani,[5] Antonella Pantaleo,[4] and Lucia De Franceschi[5]

[1]Chair of Medical Genetics, Department of Biochemistry and Medical Biotechnologies, University Federico II, Naples and CEINGE-Advanced Biotechnologies, Naples, Italy; [2]Laboratoire de Biologie et Physiopathologie des Systèmes Intégrés, FRE3094, CNRS-Université de Nice, Bâtiment de Sciences Naturelles, Nice, France; [3]Istituto di Patologia Medica, Università di Bari, Bari, Italy; [4]Dipartimento di Biochimica, Università di Torino, Italy, and [5]Department of Clinical and Experimental Medicine, Section of Internal Medicine, University of Verona, Verona, Italy

AI and LDF contributed equally to this paper.

Funding: this research was supported by the Italian Ministero dell'Università e della Ricerca, project PS 35-126/IND, Telethon (AI) and (LDF) (Italy), grants from the Convenzione CEINGE-Regione Campania-Ass. Sanità, the CNRS (Centre National de la Recherche Scientifique) and Université de Nice.

Manuscript received on October 31, 2008. Revised version arrived on March 26, 2009. Manuscript accepted on March 26, 2009.

Correspondence:
Achille Iolascon, MD, PhD, CEINGE- Advanced Biotechnologies, Via Comunale Margherita 482, 80145 Naples, Italy.
E-mail: iolascon@ceinge.unina.it

The online version of this article contains a supplementary appendix.

ABSTRACT

Background

Stomatocytoses are a group of inherited autosomal dominant hemolytic anemias and include overhydrated hereditary stomatocytosis, dehydrated hereditary stomatocytosis, hereditary cryohydrocytosis and familial pseudohyperkalemia.

Design and Methods

We report a novel variant of hereditary stomatocytosis due to a *de novo* band 3 mutation (p. G796R-band3 CEINGE) associated with a dyserythropoietic phenotype. Band 3 genomic analysis, measurement at of hematologic parameters and red cell indices and morphological analysis of bone marrow were carried out. We then evaluated the red cell membrane permeability and ion transport systems by functional studies of the patient's erythrocytes and *Xenopus* oocytes transfected with mutated band 3. We analyzed the red cell membrane tyrosine phosphorylation profile and the membrane association of the tyrosine kinases Syk and Lyn from the Src-family-kinase group, since the activity of the membrane cation transport pathways is related to cyclic phosphorylation-dephosphorylation events.

Results

The patient showed mild hemolytic anemia with circulating stomatocytes together with signs of dyserythropoiesis. Her red cells displayed increased Na^+ content with decreased K^+ content and abnormal membrane cation transport activities. Functional characterization of band 3 CEINGE in *Xenopus* oocytes showed that the mutated band 3 is converted from being an anion exchanger (Cl^-, HCO_3^-) to being a cation pathway for Na^+ and K^+. Increased tyrosine phosphorylation of some red cell membrane proteins was observed in diseased erythrocytes. Syk and Lyn membrane association was increased in the patient's red cells compared to in normal controls, indicating perturbation of phospho-signaling pathways involved in cell volume regulation events.

Conclusions

Band 3 CEINGE alters function from that of anion exchange to cation transport, affects the membrane tyrosine phosphorylation profile, in particular of band 3 and stomatin, and its presence during red cell development likely contributes to dyserythropiesis.

Key words: stomatocytosis, anion exchanger, dyserythropoiesis, tyrosine phosphorylation, Src family kinase.

Citation: Iolascon A, De Falco L, Borgese F, Esposito MR, Avvisati RA, Izzo P, Piscopo C, Guizouarn H, Biondani A, Pantaleo A, and De Franceschi L. A novel erythroid anion exchange variant (Gly796Arg) of hereditary stomatocytosis associated with dyserythropoiesis. Haematologica 2009;94:1049-1059. doi:10.3324/haematol.2008.002873

Introduction

Hereditary hemolytic disorders can be characterized by abnormal red cell morphology and perturbation of cell volume regulation. Abnormal red cells presenting a slit-like central zone of pallor on dried blood smears and named stomatocytic red cells characterize the hereditary hemolytic anemia known as stomatocytosis.[1-3] Two major forms of stomatocytosis have been delineated: overhydrated hereditary stomatocytosis and dehydrated hereditary stomatocytosis (DHSt).[2-5]

Overhydrated hereditary stomatocytosis (OMIM 185000) is generally associated with abnormal red cells characterized by altered red cell membrane permeability to Na^+ and K^+ generating swollen erythrocytes with decreased mean corpuscular hemoglobin concentration (MCHC) and increased osmotic fragility.[3] Overhydrated hereditary stomatocytosis is usually associated with the absence of the red cell transmembrane protein 7.2b, whose function is still undefined.

DHSt, also named hereditary xerocytosis (HX) (OMIM194380), is likewise characterized by abnormal red cells, which are shrunken with an increased MCHC.[2-5] Osmotic fragility is generally reduced, while autohemolysis is increased and corrected by glucose.[2-4] In DHSt/HX, the primary functional membrane defect is increased leakage of K^+ from red cells with inability of the Na-K pump to fully compensate for this leakage, so that the net intracellular cation concentration and water are decreased, leading to final red cell dehydration. In addition, in DHSt/HX red cells the increased intracellular calcium may further promote red cell water and potassium loss and cross-linking of skeletal proteins.[4,5] DHSt/HX was first described by Glader in 1974[2] and several other families have since been reported.[4-6] Clinical findings are very heterogeneous ranging from severe hemolytic anemia to symptomless disease. Analysis of all the cases showed that the unifying phenomenon is perturbation of red cell membrane leakage of univalent cations. A number of case reports on the different variants have alluded to temperature-related phenomena, including K^+ loss on storage of cells at room temperature (pseudohyperkalemia) and lysis of cells when stored at cold temperatures (cryohydrocytosis).[1]

The molecular mechanism underlying DHSt/HX has not been identified yet. Efforts have been made in the last decade to map the DHSt/HX locus: some at risk families have been collected, including a large, three-generation Irish kindred. This strategy allowed the identification of a locus on the long arm of chromosome 16 (16q23-qter) as a possible candidate. However, in a large French family of Flemish descent with familial pseudohyperkalemia (FP), microsatellite analysis excluded involvement of the 16q23-qter locus. Genome scanning mapped FP *Lille* to 2q35-36 with a Lod score of 8.46 for the D2S1338 markes. This duality suggests that the protein involved in abnormal membrane leakage may be a heterodimer.

Recently, Bruce *et al.* examined several individuals with stomatocytosis or spherocytosis associated with an increase in membrane permeability to cations, particularly marked at 0°C.[7] They found a series of single amino-acid substitutions in the intramembrane domain of erythrocyte band 3 anion exchanger (AE1), showing that these substitutions convert the protein from an anion exchanger into a non-selective cation conducter, making the scenario of stomatocytosis even more complex.[3,7,8]

Here, we report a case of hereditary stomatocytosis due to a new band 3 mutation (band 3 CEINGE), transmitted in a dominant fashion, characterized by conversion of band 3 from an anion exchanger to a cation transporter. This latter effect is associated with increased tyrosine phosphorylation of some red cell membrane proteins and increased membrane association of both Syk tyrosine kinases and Lyn tyrosine kinase, from the Src family, suggesting a pertubation of the red cell signaling pathways involved in maintaining the optimal cell volume/surface ratio. In addition, we observed signs of dyserythropiesis that make stomatocytosis due to band 3 CEINGE a novel variant of hereditary stomatocytosis.

Design and Methods

Case report

A 43-years old Caucasian female (II-2, Figure 1A) with unrelated parents was admitted to our hospital for evaluation of mild anemia. The patient had been in good health until 7 years previously when she began to experience asthenia frequently. She was first recognized to be anemic at the age of 8 years with the presence of jaundice and hyperchromic urine, but she never received blood transfusions. Bone marrow aspirate showed remarkable dyserythropoiesis with increased numbers of erythroblasts and binucleate erythroblasts, basophilic erythroblasts with alterations, irregular nuclear maturation, intererythroblastic bridges and erythroblasts with

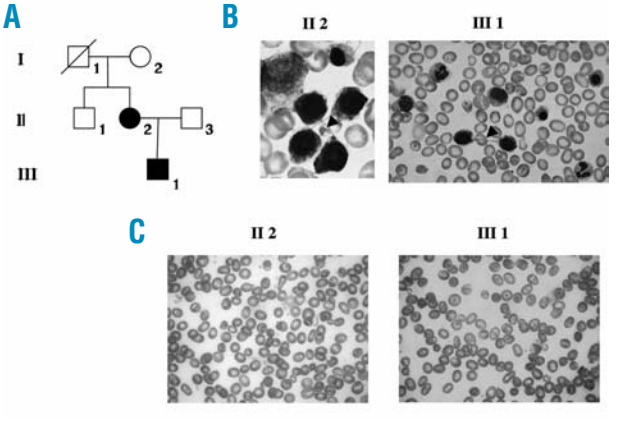

Figure 1. (A) **Family tree of proband II-2 and her son III-1. Open symbols, not affected; closed symbols, affected.** (B) **Bone marrow aspirate of proband II-2 and her son III-1 showed remarkable dyserythropoiesis with an increased number of erythroblasts and binucleate erythroblasts, basophilic erythroblasts with alterations, irregular nuclear maturation, intererythroblastic bridges (arrows) and erythroblasts with basophilic stippling.** (C) **Peripheral blood smear of proband II-2 and her son III-1 showed anisopoikilocytosis with rare stomatocytes and no spherocytes.**

basophilic stippling (Figure 1B). These bone marrow features in association with a low reticulocyte count and a low hemoglobin concentration suggested a diagnosis of congenital dyserythropoietic anemia type I.

At the age of 35 years, the patient became pregnant and she gave birth to a boy (III-1) in August 2000. Delivery was normal. At birth, the baby weighed 3,000 g and was 48 cm long. He was breastfed and was affected by anemia since infancy.

The mother and the child were admitted to our hospital for re-evaluation of their anemia.

In the mother we observed a mild hypochromic macrocytic anemia with a hemoglobin level of 11.5 g/dL, a mean cell volume (MCV) of 110 fL, and a mean hemoglobin concentration (MCH) of 36.1 pg; her reticulocyte count was 64×10^9/L. Her leukocyte count was 7.2×10^9/L with a normal differential count and her platelet count was 255×10^9/L (Table 1). She had typical hemolytic features: high levels of indirect bilirubin (3.48 mg/dL) and lactate dehydrogenase (567 U/L, normal value 240-480 U/L) and negative direct and indirect Coombs' tests. Her spleen was enlarged and ultrasonography detected a longitudinal size of 15 cm. She had undergone cholecystectomy at the age of 14 years because of numerous symptomatic small stones in the gall bladder. Serum iron, soluble transferrin receptor, serum ferritin and transferrin saturation levels were all increased (Table 1).

Other blood tests including osmotic fragility with incubated and fresh erythrocytes, serum electrolytes, B12 and folate levels, erythrocyte enzyme levels, the eosin-5'-maleimide (EMA) test and Pink test were normal.

A peripheral blood smear showed anisopoikilocytosis with rare stomatocytes and no spherocytes (Figure 1B).

The son (III-1) showed mild anemia (Hb 10.5-11.8 g/dL) with macrocytosis (MCV 101-115 fL) and hyperchromia (MCH 36.1-37 pg). Increased levels of serum iron and ferritin, transferrin saturation, soluble transferrin receptor, indirect bilirubin, and lactate dehydrogenase were detected (Table 1). His reticulocyte count, osmotic fragility tests, serum electrolytes, B_{12} and folate levels, erythrocyte enzyme levels, EMA test and Pink test were all in the normal range for the patient's age. At physical examination the spleen was enlarged.

A peripheral blood smear and bone marrow aspirate showed the same features as those observed in his mother (II-2) (Figure 1B, 1C). In particular a large number (approximately 3%) of intracytoplasmic bridges were present in the late erythroblastic stage in the bone marrow smears (Figure 1B).

After informed consent, blood was obtained for genetic analysis from the proband, her relatives, husband and son. Blood from healthy control subjects was obtained after informed consent provided according to the Declaration of Helsinki and processed within 24 h. Approval for these studies was obtained from the Federico II University Medical School institutional review board.

Nucleotide sequence analysis of CDAN1 *and* SLC4A1 *from genomic DNA*

Anticoagulated (EDTA-treated) blood samples were obtained and stored at -20°C. Genomic DNA was isolated using a QIAmp DNA Blood Mini Kit (Promega Corporation, Madison, WI, USA) according to the manufacturer's instructions.

Table 1. Hematological data of the patients (II-2 and III-1) and their parents.

	I-1	I-2	II-1	II-2	II-3	III-1	Normal values (range) male	Normal values (range) female
Hb, g/dL	15.8	14.4	13.9	11.5	14.4	11.8	12.0-17.5	12.0-16.0
WBC, $\times10^9$/L		8.64		7.2	7.38	10.1	4.8-10.8	
RBC, $\times10^{12}$/L	5.36	4.62	4.55	3.2	5.04	3.98	4.2- 5.6	4.0- 5.4
Hct, %	43	42.7	38	37.4	43	40.3	37- 54	35.0- 48.0
MCV, fL	80	92.5	83	110	85.2	105	80-97	
MCH, pg	29	31.1	30	36.1	28.5	34	25-34	
MCHC, g/dL	36	33.6	36	33	33.4	33.2	32-37	
RDW, %		12.9		20	11.3	17	11-16.5	
Reticulocyte, %	1.08	0.82	0.71	2	0.63	1.8	0.5-2	
Reticulocyte count, $\times10^9$/L	57.8	37.7	32.5	64	31.7	71.5	20- 120	
MCVr, fL		99.9		121	98.9	110.9	92.4-103	
HDWr, g/dL		3.17		4.15	2.56	4.72	2.8-4.0	
Platelet count $\times10^9$/L		363		255	290	402	130-400	
MPV, μm^3		9.4		9.5	9.85	7.06	7.1-10	
Indirect bilirubin, mg/dL	0.38		0.5	3.48		2.7	0.98-0.75	
Ferritin, µg/L		146		440		78	18-370	9-120
Serum iron, µg/dL	55	113	118	145		106	16-124	
Transferrin, mg/dL		277		152		230	174-446	
Transferrin saturation, %		31.3		68.5		58.8	15- 35	
Soluble transferrin receptor, mg/L		0.91		3.36		9.58	0.83-1.16	

Hb: hemoglobin; WBC: white cell count; RBC: red cell count; Hct: hematocrit; RDW: red cell distribution width; MPV: mean platelet volume; HDWr: reticulocyte hemoglobin distribution width.

To screen for mutations of codanin gene (*CDAN1*) in the patients (mother and son), each of the 28 exons with exon-intron boundaries were amplified by polymerase chain reaction (PCR) using specific primers. PCR fragments were sequenced directly. A similar approach was used to analyze the *SLC4A1* gene: all coding exons, including splice junctions, and portions of the promoter region were amplified by PCR. The amplified products were isolated by electrophoresis on 1% agarose gel and purified using a QIAamp purification kit (Qiagen, Valencia, CA, USA). Direct sequencing was performed using a fluorescence-tagged dideoxy chain terminator method in an ABI 310 automated sequencer (Applied Biosystem, Foster City, CA, USA), according to the manufacturer's instructions. Primers used for PCR and sequencing and PCR conditions are available on request. The *CDAN1* and *SLC4A1* cDNA sequences from GenBank accession numbers NC_000015.8 and NC_000017.9, respectively, were used as reference sequences.

We investigated the identified *SLC4A1* mutation in DNA samples from 50 healthy white controls (100 chromosomes). We sequenced the amplified exon 17 using the following primers: sense 5'-ttattcccagccccagata-3' and antisense 5'-acttattcacgggcatccag-3'.

Red cell membrane protein analysis

Red-cell ghosts were prepared according to the procedure of Dodge *et al*.,[9] except that 5 mM phenylmethylsulfonyl fluoride was added during the lysis step (for details see also *Online Supplementary materials*).

Measurements of red cell cation content and Na/K pump, Na/K/2Cl, K/Cl co-transport and Na/H exchange activities in red cells

The erythrocyte content of Na^+ and K^+ was determined by an atomic absorption spectrometer (ANALYST 2000, Perkin-Elmer, Branchberg, NJ, USA) using standards in double-distilled water. Cation transport activities were estimated according to previously published methods.[10,11] Briefly, the maximal rates of Na/K pump and Na/K/Cl co-transport activities were measured in cells containing equal amounts of Na^+ and K^+ (50 mmol/L of cells, obtained with the nystatin technique). With this procedure the internal sites for both transport systems were saturated.[10,12,13] The nystatin loading solution contained 70 mmol/L NaCl, 70 mmol/L KCl and 55 mmol/L sucrose. The Na/K pump activity was estimated as the ouabain-sensitive fraction of Na^+ efflux into a medium containing 130 mmol/L choline chloride and 10 mmol/L KCl. The ouabain concentration was 0.1 mmol/L. Na/K/Cl/ co-transport was estimated as the bumetamide-sensitive fraction of Na^+ efflux into a medium containing 140 mmol/L choline chloride and 0.1 mmol/L ouabain. The bumetamide concentration was 0.01 mmol/L. All media contained 1 mmol/L $MgCl_2$, 10 mmol/L glucose, and 10 mmol/L Tris-MOPS pH 7.4. The Na/H exchange rate was evaluated as the amiloride-sensitive Na^+ efflux stimulated by hypertonic shrinkage from cells containing equal amounts of Na^+ and K^+.[10,14] The media contained 140 mmol/L choline chloride and the osmolarity was increased with sucrose. 5-N,N hexamethyleneamiloride, at a final concentration of 10 mmol/L, was used as a specific inhibitor of the system.[10,12,13]

Red cell membrane protein tyrosine phosphorylation profile and immunoblot analysis

Red-cell ghosts separated by one-dimensional electrophoresis were solubilized by Sample Buffer (SB: 50 mmol/L Tris, pH 6.8, 100 mmol/L β-mercaptoethanol, 2% v/v SDS, 10% v/v glycerol, and a few grains of bromophenol blue), and loaded on either 10% or 8% gel. The gels were either stained with colloidal Coomassie or transferred to membranes for immunoblot analysis and probed with either specific anti-phosphotyrosine antibodies (PY99-clone SantaCruz Biotechnology, CA, and 4G10-clone, UpState, NY, USA) or anti-Lyn antibody (Santa Cruz Biotechnologies, Santa Cruz, CA, USA), and anti-Syk antibody (Cell Signaling, Danvers, MA, USA).[11]

To evaluate whether cell swelling induced changes in the tyrosine-phosphorylation profile of red cell membrane proteins, control red cells were incubated with and without urea (600 mmol/L final concentration) as previously described by Joiner *et al*.[15] and red-cell ghosts were prepared for immunoblot analysis with specific antiphosphotyrosine antibodies. In some experiments tyrosine-enriched proteins were obtained by immunoprecipitation with a specific anti-phosphotyrosine antibody (clone 4G10, UpState, NY, USA) as previously reported by De Franceschi *et al*.[16,17] Briefly, red-cell ghosts were solubilized in a medium containing 50 mmol/L Tris-HCl, pH 7.4, 100 mmol/L NaCl, 5 mmol/L EDTA, 1% Triton X-100, 1 mmol/L Na- orthovanadate, 0.004% benzamidine, and 1 tablet of a protease inhibitor cocktail (Roche, Germany). After incubation for 60 min at 4°C, the protein extract was centrifuged at 15,000 g for 15 min and the supernatant was used for immunoprecipitation. Anti-phosphotyrosine (clone 4G10) was used to immunoprecipitate tyrosine-phosphorylated proteins with protein A-Trysacryl followed by washing. The immunoprecipitated proteins were then either used for immunoblot analysis with specific anti-β spectrin antibody (clone 4C3, Acris Hiddenhousen, Germany), anti-band 3 antibody (clone IVF12, DSHB, Iowa City, Iowa, USA), anti-stomatin antibody (a kind gift from R Prohaska, Wein University, Wein, Austria) or stained with colloidal Coomassie for protein identification as previously described.[11] Secondary antibodies were from GE Healthcare (Little Chalfont, UK). ECL-Plus (Amersham, UK) was used as the revealing system.

Protein identification

The selected bands were identified by MALDI-TOF MS/MS analysis and automated LC-MS/MS analysis. Mass spectrometric analysis was performed using a Tofspec SE (Micromass, Manchester, UK). Peptide spectra were obtained in positive ion mode over the m/z range of 800-4000 Da or 1000-3000 Da in reflectron mode. The peptide solution was prepared by mixing equal volumes of matrix (matrix: saturated α-cyano-4-hydroxy cynnamic acid solution in 40% acetonitrile, 60% of 0.1% trifluor acetic acid). Between 100-120 laser shots were summed for each MS spectrum. The meas-

ured peptide masses were searched for in the Swiss-Prot database (taxa human) using the MASCOT search engine (Matrix Science Ltd., London, UK). Only protein identifications with a significant Mascot score ($p<0.05$) were taken into consideration. A mass accuracy of 0.3 Da and a single missed cleavage were allowed for each matching peptide. Searches were not constrained by pI or molecular weight.[11,18] Peptide mixtures were also analyzed using microflow capillary liquid chromatography coupled with electrospray quadrupole time of flight tandem mass spectrometry (ESI Q-TOF MS/MS). ESI-MS/MS tandem spectra were recorded in the automated MS to MS/MS switching mode, with an m/z-dependent set of collision offset values. Singly to quadruply charged ions were selected and fragmented, using argon as the collision gas. External calibration was performed with a solution of H_3PO_4 0.05% in H_20/MeCN 50/50. Mass data collected during RP-LC-MS/MS analysis were processed and converted into a PKL file to be submitted to the automated database searching *Mascot, MS/MS Ions Search*. Search parameters were: parent tolerance 0.6 Da, fragment tolerance 0.3 Da, tryptic specifity allowing for up to one missed cleavage, database SWISSPROT.

Plasmid preparation and studies in oocytes

Point mutations to get a G796R substitution on erythroid human AE1 (eAE1) were made by PCR using the Quick change site-directed mutagenesis kit from Stratagene with the following forward primer: G796R : ATCTTCCTCTACATGAGGGTCACGTCGCTCAGC and reverse primer: GCTGAGCGACGTGACCCT-CATGTAGAGGAAGAT. One positive clone was entirely sequenced before further use. pSP65 eAE1 was a gift from Dr. Appelhans.

Oocytes were harvested from anesthetized female *Xenopus laevis* according to the procedure recommended by the ethical committee of the CNRS (Centre National de la Recherche Scientifique).

Oocytes were defolliculated as previously described[9] with overnight incubation in 2 mg/mL collagenase NB4 Serva (Heidelberg, Germany) and 30 min incubation in Ca^{2+} free medium. Stage V-VI oocytes were selected for cRNA injection. cRNA were prepared from cDNA using a SP6 transcription kit from Ambion (Huntingdon, UK). The concentration and quality of cRNA were determined by OD measurements and with formamide/formaldehyde agarose gel in MOPS (3-[N-morpholine]propanesulfonic acid) buffer. Ten nanograms of wild type or mutant eAE1 cRNA were injected per oocyte. Oocytes were kept in MBS (Modified Barth Saline) consisting of NaCl 85 mmol/L; KCl 1 mmol/L; $NaHCO_3$: 2.4 mmol/L; $MgSO_4$ 0.82 mmol/L; $Ca(NO_3)_2$ 0.33 mmol/L; $CaCl_2$ 0.41 mmol/L; HEPES (N-2-hydroxyethlylpiperazine-N-2-ethanesulfonic acid) 10 mmol/L; NaOH 4.5 mmol/L; pH 7.4 supplemented with penicillin (10 U/mL) and streptomycin (10 µg/mL).

Lithium was used as a substitute for sodium to measure oocyte cation permeability. Oocytes (7 per condition) were incubated for 2 h at 19°C in MBS in which NaCl was substituted by $LiNO_3$, for a final composition of $LiNO_3$ 85 mmol/L; KNO_3 1 mmol/L; $KHCO_3$ 2.4 mmol/L; $MgSO_4$ 0.82 mmol/L; $Ca(NO_3)_2$ 0.33 mmol/L; $CaCl_2$ 0.41 mmol/L; HEPES 10 mmol/L; NaOH 4.5 mmol/L; pH 7.4. In addition, oubain (0.5 mM) and bumetanide (5 µM) were added to block Na^+/K^+ pump activity and Na^+-K^+-$2Cl^-$ co-transport. Oocytes were rinsed three times in milliQ H_2O and placed one by one in a tube heated at 95°C to desiccate them. Intracellular lithium was extracted by addition of 50 µL 0.1N NaOH and further diluted by addition of 250 µl milliQ H_2O. The lithium content in each oocyte extract was measured by atomic absorption spectrometry with a Perkin Elmer AAS 3110 (Perkin-Elmer, Branchberg, NJ, USA). Data are the means ± s.e.m. of 112 oocytes (non-injected), 70 oocytes (wild type eAE1), and 21 oocytes (G796R).

After injection, oocytes were incubated at 19°C for 3 days in MBS with oubain (0.5 mM) and bumetanide (5 µM) to prevent any Na^+ or K^+ recycling or movement through the Na^+/K^+ pump or Na^+-K^+-$2Cl^-$ co-transporter. For each condition and experiment, three sets of five oocytes were quickly rinsed twice in milliQH_2O and dried overnight at 80°C. Intracellular cations were extracted from dried oocytes by overnight incubation in 4 mL of milliQ H_2O. Na^+ and K^+ were quantified by flame photometry (Eppendorf AG, Hamburg, Germany). Data, expressed in µmol per gram of dry weight, are the means of two different experiments ± s.e.m. (n=6).

Oocyte intracellular pH was measured using selective microelectrodes as previously described.[9] The ability of wild type eAE1 and mutant G796R to regulate intracellular pH was assessed by measuring intracellular pH of oocytes adapted in MBS without HCO_3^- then incubated in the following medium: NaCl 63.4 mmol/L; KCl 1 mmol/L; HCO_3^- 24 mmol/L; $MgSO_4$ 0.82 mmol/L; $Ca(NO_3)_2$ 0.33 mmol/L; $CaCl_2$ 0.41 mmol/L; HEPES/NaOH 5 mmol/L pH 7.35; CO_2 5%, O_2 95% and then bathed in MBS without Cl (Na gluconate 63.4 mmol/L; K gluconate 1 mmol/L; HCO_3^- 24 mmol/L; $MgSO_4$ 0.82 mmol/L; $Ca(NO_3)_2$ 0.74 mmol/L; HEPES/NaOH 5 mmol/L; pH 7.35, CO_2 5%, O_2 95%). Traces are representative of three oocyte recordings for each condition.

Results

Genomic analysis

Based on the patient's history and hematologic data, we first considered the possibility of congenital dyserythropoietic anemia type I, related to a codanin-1 mutation. We sequenced the *CDAN1* gene without finding mutations in either the mother or her son (*data not shown*). The absence of any clinical signs of anemia during the neonatal period and the lack of skeletal malformations in both subjects, associated with the absence of any detectable mutation in the codanin gene led us to exclude congenital dyserythropoietic anemia type I as the cause of our patients' anemia.

The increased red cell MCV and the dominant inheritance pattern led us to consider hereditary stomatocytoses, which are associated with hemolytic anemia, macrocytosis, and abnormally shaped red blood cells

(stomatocytes) (Figure 1C). We investigated the gene encoding for the red cell membrane protein band 3 (*SLC4A1*), which is one of the genes involved in hereditary stomatocytosis.[8] We screened the *SLC4A1* coding sequence and exon-intron junctions for mutations by direct sequencing and identified a G>A transition at nucleotide 2500 in exon 17 (Figure 2A) in both the proband and in her son in the heterozygous state. No mutation was found in the grandmother; DNA from the grandfather was not available. The mutation identified changes the GGG codon to AGG, causing the substitution of glycine 796 with arginine (p.G796R) in band 3 protein. This novel mutation does not create or abolish any enzyme restriction site, so we analyzed 50 controls (100 chromosomes) by direct sequencing of exon 17. None of the control population had the mutation, suggesting that this gene defect is causative of this anemia and is not a genetic polymorphism (*data not shown*). In addition, by using PROGRAM blastn-SNP (*http://www-btls.jst.go.jp/cgibin/Homology_Blast-SNP/submission_v3.cgi?PROGRAM_blastn-SNP*), we excluded that this nucleotide change corresponds to a previously identified single nucleotide polymorphism.

Glycine 796 is perfectly conserved in mammals as well as in other species, suggesting that it has an essential role in the structure and function of band 3 (see also *Online Supplementary materials*, Figure 2B). In transmembrane segments glycine is often located at helix-helix interfaces allowing close packing (see *Online Supplementary Figure S1*). The G796R mutation would introduce a positive charge and could seriously disrupt helix packing.

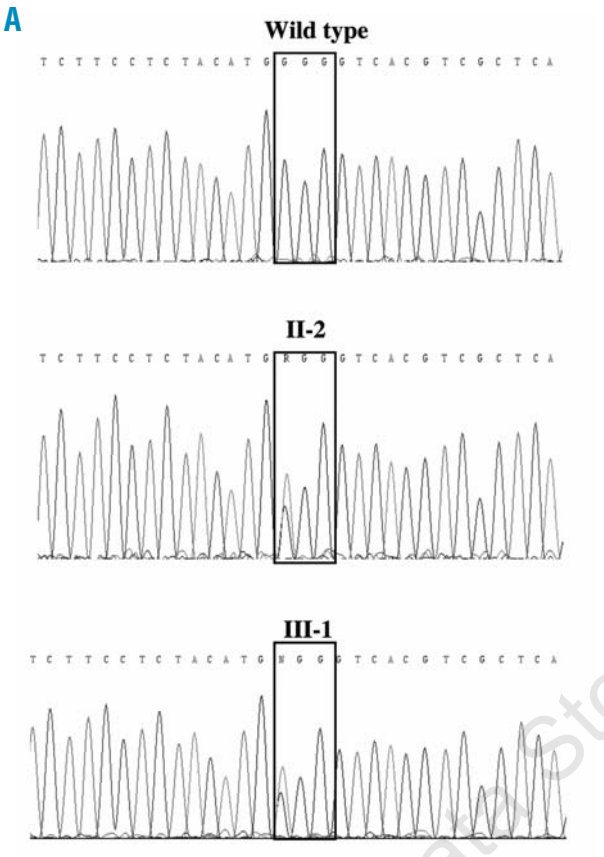

Figure 2. (A) **Identification of the *SLC4A1* mutation in II-2 and III-1. Partial sequence of exon 17 of the proband and wild-type DNA identifying the G>A transition at nucleotide 2500. The mutation changes the GGG codon to AGG, causing the substitution of glycine 796 with arginine (p. G796R) in the protein (boxed).** (B) **Alignment analysis of the amino acid sequences of *SLC4A1* (Band 3) from different species, showing complete conservation of the G796 residue (boxed).**

B

	792											800								
Homo sapiens	L	F	G	I	F	L	Y	M	G	V	T	S	L	S	G	I	Q	L	F	D	R	**808**
Pongo abelii	L	F	G	I	F	L	Y	M	G	V	T	S	L	S	G	I	Q	L	F	D	R	**749**
Canis Familiaris	L	F	G	I	F	L	Y	M	G	V	T	S	L	S	G	I	Q	L	F	D	R	**826**
Pan troglodytes	L	F	G	I	F	L	Y	M	G	V	T	S	L	S	G	I	Q	L	F	D	R	**797**
Mus musculus	L	F	G	I	F	L	Y	M	G	V	T	S	L	S	G	I	Q	L	F	D	R	**826**
Rattus norvegicus	L	F	G	I	F	L	Y	M	G	I	T	S	L	S	G	I	Q	L	F	D	R	**825**
Equus caballus	L	F	G	I	F	L	Y	M	G	V	T	S	L	S	G	I	Q	F	F	D	R	**830**
Bos taurus	L	F	G	I	F	L	Y	M	G	V	T	S	L	S	G	I	Q	L	F	D	R	**826**
Monodelphis domestica	L	F	G	I	F	L	Y	M	G	V	T	S	L	S	G	I	Q	L	F	D	R	**949**
Gallus gallus	L	F	G	I	F	L	Y	M	G	V	T	S	L	S	G	I	Q	L	F	D	R	**819**
Macaca mulatta	L	F	G	I	F	L	Y	M	G	V	T	S	L	N	G	I	Q	F	Y	E	R	**1069**
Danio rerio	L	F	G	I	F	L	Y	M	G	V	T	S	L	S	G	I	Q	L	F	D	R	**1129**
Leucoraja erinacea	L	F	G	I	F	L	Y	M	G	V	T	S	L	S	G	I	Q	L	F	D	R	**1114**
Tetraodon nigroviridis	L	F	G	I	F	L	Y	M	G	V	T	S	L	S	G	I	Q	L	F	D	R	**1181**
Drosophila melanogaster	L	F	G	V	F	L	Y	M	G	V	T	S	L	S	G	I	Q	L	F	D	R	**1101**
Xenopus laevis	L	F	G	I	F	L	Y	M	G	V	T	S	L	S	G	I	Q	L	F	D	R	**923**
Caenorhabditis elegans	L	Y	G	V	F	L	Y	M	G	I	S	A	L	G	G	I	Q	L	F	D	R	**922**
Saccharomyces cerevisiae	L	S	G	L	F	F	I	M	G	I	N	G	L	M	T	N	S	I	I	Q	R	**471**

Fluorescent binding studies and protein membrane composition of red blood cells

We then evaluated the amount of mutated band 3 in the red cell membrane. Band 3 red cell membrane content was quantified using two separate methods: by flow cytometry of EMA-labeled red cells and by sodium dodecyl sulphate-polyacrylamide gel electrophoresis (SDS-PAGE) analysis. Previous studies have shown that the intensity of fluorescence detected by fluorescence microscopy following EMA binding is directly proportional to the abundance of cellular band 3 protein.[19] We compared EMA-labeled red cells from patients II-2 and III-1 and normal controls and did not observe significant differences, indicating neither deficiency nor defective band 3 protein in diseased red cells (*data not shown*). In addition, SDS-PAGE analysis did not show any major changes in red cell membrane band 3 content or in other cell membrane proteins, so we further excluded hereditary spherocytosis but also congenital dyserythropoietic anemia type II (*data not shown*).

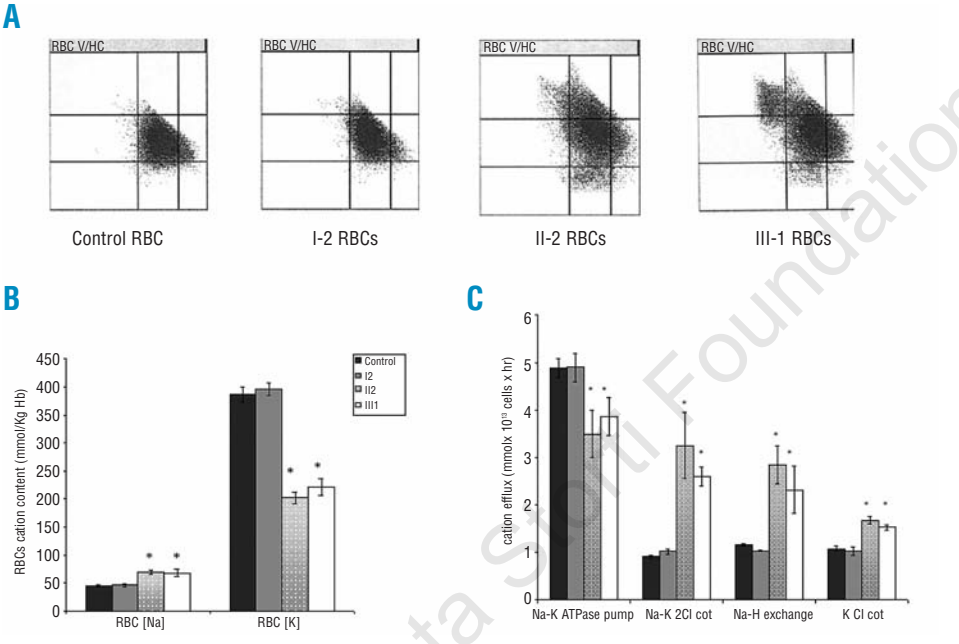

Figure 3. (A) Erythrocyte cation content and membrane cation transport pathways. Red blood cell histograms generated for erythrocyte volume (RBC V) and cell hemoglobin concentration (RBC HC) and plot of RBC HC (*x-axis*) *vs.* RBC volume (*y-axis*) from control red blood cells (RBC) and from I-2, II-2 and III-1 are presented. (B) Red cell Na^+ and K^+ contents in normal controls (black bar) and in subjects I-2 (dark gray bar), II-2 (light gray bar) and III-1 (white bar). Data are reported as means±SD (controls; n=6, I-2, II-2, III-1 n= 3) *p<0.05 compared to control red cells. (C) Cation transport pathways in red cells from normal controls (n=6) and subjects I-2 (dark gray bar), II-2 (light gray bar) and III-1 (white bar). Data are expressed as means ± SD (controls; n=6; I-2, II-2, III-1 n=3); *p<0.05 compared to control red cells.

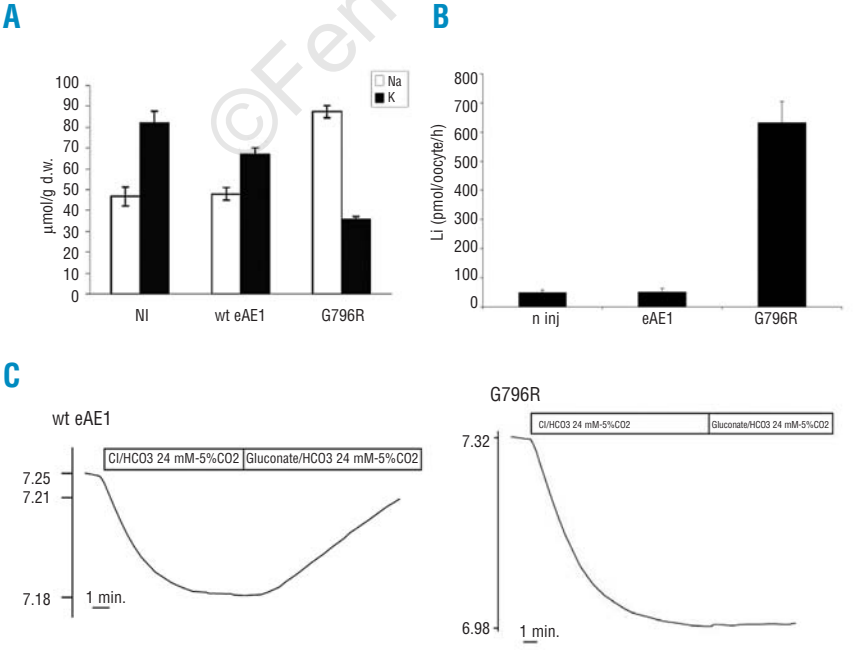

Figure 4. (A) Cation transport properties of the G796R mutation. Intracellular Na^+ and K^+ contents of oocytes non-injected (NI) or expressing wt eAE1 or G796R eAE1 mutation 3 days after injection. Oocytes had been kept in MBS with 0.5 mM ouabain and 5 µM bumetanide. Results are expressed in µmol per g of dry weight, means±s.e.m., n=6. There was no statistically significant difference in cation contents between NI and wt eAE1. p<0.005 for G796R mutant compared to wt eAE1. (B) Lithium influx: oocyte Li^+ uptake was measured during the linear phase of kinetics in MBS in which Na^+ was substituted by Li^+ (see Design and Methods), in the presence of 0.5 mM ouabain and 5 µM bumetanide. Oocytes were non-injected (NI) or expressed wt eAE1 or G796R eAE1 mutation for 3 days. Data are means±s.e.m. (C) pHi recordings: intracellular pH in oocytes expressing wt eAE1 or G796R mutation as a function of extracellular medium. Representative traces (n=3). The slope of the acidification as well as the pHi value at plateau differ significantly between wt and mutant AE1 due the ability of wt eAE1 to compensate the acidification induced by CO_2 uptake.

Erythrocyte cation content and membrane cation transport pathways

The fact that the MCV and hemoglobin distribution width of reticulocytes from II-2 and III-1 were increased (Table 1 and Figure 3A) suggested that abnormalities in red cell volume regulation were already present in reticulocytes and were not related to the permanence of red cells in the peripheral circulation.

Cell Na^+ content was significantly higher in red cells from II-2 and III-1 than in those from I-2 and controls, while red cell K^+ content in II-2 and III-1 was significantly lower than in I-2 and control erythrocytes, indicating a reduction in total red cell cation content similarly to what has been observed in other cases of dehydrated hereditary stomatocytosis (Figure 3B).[20] Since previous reports suggested a possible functional relationship between red cell membrane proteins and cation transport pathways,[13,14,18,19] we evaluated the activity of the main cation transport pathways in normal and diseased red cells. We observed a significant decrease in the activity of the Na-K ATPase pump in II-2 and III-1 compared to the level in I-2 and in control erythrocytes, suggesting a perturbation in Na-K pump ATPase in our anemic subjects; Na-K-2Cl co-transport, K-Cl co-transport and Na-H exchange were significantly increased in II-2 and III-1 compared to in I-2 and in control erythrocytes (Figure 3C).

Functional studies of band 3 CEINGE in oocytes

To investigate the ion functional properties of the G796R mutation, *Xenopus* oocytes were injected with control eAE1 (wild type erythroid anion exchanger 1: wt eAE1) or G796R-eAE1. Whole cell membrane preparations of wild type or mutated AE1 were loaded on an electrophoresis gel. Immunodetection showed similar patterns of expression between the two proteins (*Online Supplementary Figure S2*). As in red cells G796R was correctly addressed to the plasma membrane, there being no indication to suspect a fault in G796R expression in oocytes. The Na^+ and K^+ contents of oocytes were measured 3 days after injection and the cation permeability was also assessed by measuring Li^+ influx. To prevent cation movements through the Na-K-ATPase and the endogenous Na-K-2Cl co-transporter, measurements were done in the presence of their specific inhibitors, ouabain and bumetanide. Whereas wt eAE1 did not change oocyte Na^+ and K^+contents, which were similar to those in control oocytes (NI) (Figure 4A), the G796R mutation induced a reversal of Na^+ and K^+ oocyte contents. There was a net Na^+ uptake of 39±6 μmol/g d.w. compensated by a similar net K^+ loss of 31±4 μmol/g d.w. ($p<0.005$ versus wt eAE1). These changes in oocyte cation contents were associated with increased cation permeability (Figure 4B). The cation transport induced by the G796R mutation was not sensitive to 0.1 mmol/L SITS (*data not shown*), in contrast to previously studied AE1 point mutations also inducing cation transport through the anion exchanger.[7,21]

The Cl^-/HCO_3^- exchange activity of G796R mutation was also assessed. Oocyte intracellular pH was recorded as a function of extracellular medium. In medium buffered with 24 mM HCO_3^-/5% CO_2 the rapid CO_2 equilibration through oocyte plasma membrane induced intracellular acidification. Then, in this medium Cl^- was substituted by gluconate, an anion to which the oocytes are impermeable. In the presence of functional Cl^-/HCO_3^- exchange, this condition induced rapid intracellular alkalinization. Figure 4C shows representative pHi recordings of oocytes expressing wt eAE1 or G796R mutant. Following intracellular acidification, oocytes expressing wt eAE1 alkalinized in the absence of extracellular Cl^-. In contrast, oocytes expressing G796R mutant did not recover from the initial acidification. We also carried out experiments in the presence of co-injected glycophorin A which did not modify the cation transport properties of the mutated band 3 (*data not shown*). Thus, the band 3 point mutation G796R abolishes anion exchange activity whereas it induces Na^+ and K^+ transport.

Tyrosine phosphorylation pattern of red cell membrane and tyrosine kinase Syk and Lyn membrane association

Since changes in protein tyrosine phosphorylation state have been shown to be involved in the modulation of membrane transport and channels involved in cell vol-

Table 2. Identification of proteins differently phosphorylated from those of the patient's red cell membrane.

#	AC	Protein	Matching peptide	Coverage (%) residues (STY)	Phosphorylated		Phosphorylated peptides
			MALDI-TOF				MS/MS
					75	83	(R)ITDLYKDLR(D)
					380	387	(K)VYTPHDGK(L)
1	P11277	Spectrin β	120	48	509	521	(R)LWSYLQELLQSRR(Q)
					594	611	(K)FTEGKGYQPCDPQVIQDR(M)
2	P16157	Ankyrin	35	22	733	755	(K)LGYSPLHQAAQQGHTDIVTLLLK(N
3	P02730	Band 3	20	21	346	360	(R)RYQSSPAKPDSSFYK(G)
4	P11171	Band 4.1	14	23	451	466	(K)IRPGEQEQYESTIGFK(L)
5	P16452	Band 4.2	12	18	654	673	(R)LDGENIYIRHSNLMLEDLDK(S)
6	P60709	Actin β	9	29	178	191	R.LDLAGRDLTDYLMK.I
					184	196	R.DLTDYLMKILTER.G
7	P27105	Stomatin	12	41	nd		nd

The corresponding bands are indicated in Figure 5; nd: not identified.

ume regulatory events,[22-24] we evaluated the red cell membrane tyrosine phosphorylation profile in II-2 and III-1. As shown in Figure 5A, membrane tyrosine phosphorylation was markedly increased in the affected subjects compared to in normal controls.

In order to evaluate whether changes in the tyrosine-phosphorylation pattern of red cell membrane proteins were part of the physiological response to a cell swelling stimulus, we incubated normal erythrocytes with and without urea and then evaluated the red cell membrane tyrosine-phosphorylation profile.[15] In urea-treated red cells, we observed increased tyrosine-phosphorylation of proteins with a molecular weight greater than 181 KDa, one band between 181-115 KDa and one at 82 KDa which were also found in diseased red cells (bands 1, 2, 3; Figure 5A), suggesting a possible adaptive mechanism of red cells to swelling involving these proteins. However, in diseased red cells we observed additional changes in tyrosine phosphorylation state of other membrane proteins, indicating an independent effect of the hematologic phenotype (Figure 5A). In order to identify the erythrocyte membrane proteins differently tyrosine-phosphorylated, we analyzed anti-phosphotyrosine immunoprecipitated proteins separated by one-dimensional electrophoresis (Figure 5B). Bands that were differently tyrosine phosphorylated were excised and analyzed by mass spectrometry. We identified the following proteins: β spectrin, ankyrin, band 3, band 4.1, band 4.2, β actin and stomatin (Table 2). We then evaluated the amount of β spectrin, band 3 and stomatin on anti-phosphotyrosine immunoprecipitated proteins separated by one-dimensional electrophoresis (Figure 5B). We observed a slightly increased amount of β spectrin in diseased red cells compared to in normal controls but a marked increase of both band 3 and stomatin compared to in control erythrocytes (Figure 5B). These data suggest that the mutated band 3 might affect membrane organization either directly favoring the exposure of phosphorylable docking sites on red cell membrane proteins or indirectly through activation of signal transduction pathways related to abnormal red cell volume/surface ratio (Figure 5). Since band 3 is a known substrate for both Syk tyrosine kinase and Lyn tyrosine kinase of the Src family,[21-23] we evaluated the amount of both tyrosine kinases bound to the membrane in red cells from both patients and controls. As shown in Figure 5C, Syk and Lyn kinase membrane association was markedly higher in patients' red cells than in normal controls, most likely being responsible for the increased band 3 tyrosine-phoshorylation state in patients' red cells.

Discussion

Here, we report a case of hereditary stomatocytosis due to a *de novo* band 3 mutation (p. G796R) associated with signs of dyserythropoiesis. Band 3 is a 911 amino-acid multispanning membrane protein that conducts bicarbonate-chloride exchange in red cells. Mutations in the band 3 gene resulting in a decrease of band 3 protein in red cells are frequent causes of hereditary spherocytosis. Deletion of 400-408 amino acids near the first transmembrane domain causes Southeast-Asian ovalocytosis. Red cells from patients with this condition have been shown to leak cations at low temperature, this phenotype justifying the inclusion of Southeast-Asian ovalocytosis in the group of hereditary stomatocy-

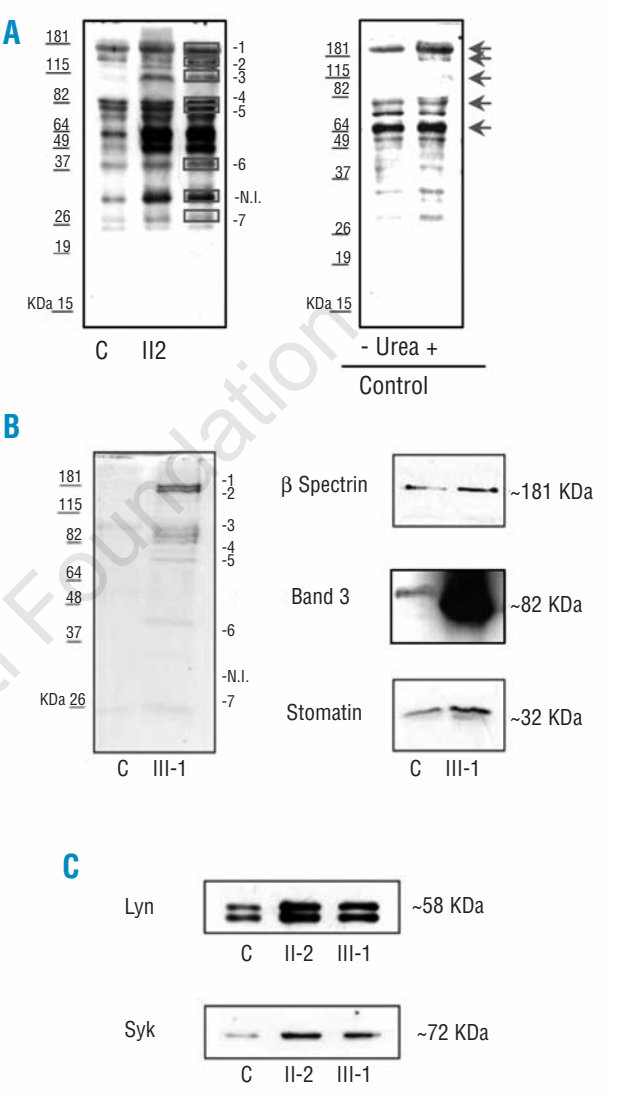

Figure 5. (A) **Tyrosine phosphorylation profile of red cell membrane from controls (C), II-2 and III-1 and effects of cell swelling induced by urea on control erythrocytes. Red cell ghosts were separated by one-dimensional electrophoresis and blotted with specific anti-phosphotyrosine antibodies to evaluate the tyrosine phosphorylation pattern of red cell membrane proteins. One out of three independent experiments with similar results is presented. (B) Red cell ghosts underwent immunoprecipitation with specific anti-phosphotyrosine antibodies and were then used for immuno-blot analysis with specific anti-β spectrin antibody, anti-band 3 antibody and anti-stomatin antibody. One out of three independent experiments with similar results is presented. The red boxes in panel A and the red lines in panel B indicate the identified proteins (see Table 2); the red arrows indicate the bands differently tyrosine-phosphorylated in urea-treated normal red cells with behavior similar to those observed in diseased erythrocytes; ni: protein not identified. (C) Immunoblot analysis with anti-Syk and anti- Lyn antibodies of red cell ghosts from controls (C) and from II-2 and III-1. Gels were loaded with the same amount of proteins used in the colloidal Coomassie-stained gel shown in the upper part of the panel. One out of three independent experiments with similar results is presented.**

toses.[3,4] Mutations in the 9-10th membrane spanning domains are associated with hereditary cryo-stomatocytosis and cation leak. The present *de novo* mutation is located in this latter area and causes the same effect on cation leak, but appears to be associated with some dyserythropoietic features.

Hereditary stomatocytoses can be classified in dehydrated hereditary stomatocytosis, overhydrated hereditary stomatocytosis, hereditary cryo hydrocytosis and familial pseudohyperkalemia. In our case there was no pseudohyperkalemia, and the ion content was similar to that in hereditary cryohydrocytosis. Thus, it could be considered a variant of hereditary cryohydrocytosis because the reticulocyte count was associated with several dyserythropoietic findings, as supported by the low reticulocyte count, bone marrow abnormalities and increased soluble transferrin receptor but near normal hemoglobin content (Table 1). A literature review of hereditary stomatocytosis revealed two case reports with similar findings. One case had mild anemia, increased MCV, slightly reduced red cell K^+ content and normal Na^+ content, reduced reticulocyte count with respect to the anemia and alterations of erythroid progenitors in bone marrow consistent with atypical congenital dyserythropoietic anemia type I. The red cell membrane showed reductions of band 7 and 8 on SDS-PAGE analysis.[25] The second case, reported by Jarvis *et al.*, had an abnormal intracellular cation content and increased MCV, inherited in a dominant manner, interestingly due to a *de novo* mutation. Unfortunately, the biochemical and molecular defects were not reported.[26] Evidence of connections between dyserythropoiesis and band 3 mutation has been recently found in zebrafish mutant retsina (ret), which is characterized by band 3 mutations associated with an erythroid-specific defect in cell division causing marked dyserythropoiesis similar to that occurring in human congenital dyserythropoietic anemia.[27] In our cases we observed dyserythropoiesis characterized by a large number of intracytoplasmic bridges (approximately 3%) between late erythroid precursors, suggesting a possible role of mutated band 3.

Recently the analysis of 11 human pedigrees with dominantly inherited hereditary stomatocytosis (hereditary cryohydrocytosis subtype) and hereditary spherocytosis has shown an increased membrane permeability to Na^+ and K^+, related to a series of single amino acid substitutions in the band 3 anion exchanger, characterized by a conversion of the mutated band 3 function from an anion exchanger into a non-selective cation leaker.[8,9] We, therefore, searched for band 3 mutations and identified a G>A transition at nucleotide 2500 in exon 17 (Figure 2A) in the proband and in her son in the heterozygous state. This molecular *bona-fide* event was due to a *de novo* mutation since the red cell MCV of the proband's parents was normal. Functional studies showed that mutated band 3 converted the anion exchanger (Cl^-, $HCO3^-$) function to a cation pathway for Na^+ and K^+.

The patients' red cells showed abnormal cation content, associated with decreased Na-K pump activity, most likely related to metabolic alterations already described in stomatocytosis,[28] but also increased Na-K-2Cl co-transport activity which is strictly dependent on the intracellular Na^+ content, and may contribute to the net Na^+ extrusion from diseased red cells. The Na-H exchange and K-Cl co-transport might be secondarily activated either by possible abnormal functional interactions between membrane proteins and the transmembrane ion transport pathway or by perturbations in signal transduction pathways modulating ion movements through the membrane, as previously described in mouse red cells genetically lacking band 4.1.[10,29] Since the activity of the membrane cation transport pathways is related to cyclic phosphorylation-dephosphorylation events by kinase phosphatases, we evaluated the membrane tyrosine phosphorylation profile in diseased red cells. In diseased red cells, we observed an increase of band 3 tyrosine phosphorylation, most likely due to increased membrane association of Syk and Lyn kinases which have already been reported to tyrosine-phosphorylate band 3.[30-32] In addition, changes in the tyrosine-phosphorylation of band 4.1, band 4.2, and stomatin were evident in diseased red cells and were independent of the adaptive mechanisms to cell swelling (Figure 5), suggesting a perturbation of intracellular signaling pathways toward the membrane-cytoskeleton network.[22,33-35] Previous studies in skate red cells have shown that volume expansion is associated with increased Syk and Lyn activity and changes in phosphorylation state of various membrane proteins and in their association with membrane lipid rafts.[22,35,36] Here, it is of interest to note that the patients' red cells showed increased tyrosine-phosphorylation of stomatin, which is the major protein in lipid rafts; changes in tyrosine-phosphorylation state of stomatin may affect its conformational state and function, most likely contributing to the red cell phenotype.[37,38]

These finding, together with the demonstration of the causative role of this band 3 mutation, led us to classify this case as stomatocytosis, but as a novel variant because of the lack of appearance of anemia in the neonatal period, normal or reduced reticulocyte count and normal hemoglobin level in the mother and her affected son. In addition, the reduced reticulocyte count and appearance of the bone marrow erythroid compartment supported our conclusion that this is a new variant of stomatocytosis with several dyserythropoietic features.

Authorship and Disclosures

AI obtained institutional review board approval and consent, designed and conducted studies and prepared the manuscript; LDF performed DNA and red cell membrane analyses; FB and HG performed oocyte studies; RAA and MRE performed red cell membrane analyses; PI and CP contributed to the clinical care of the patients and to morphological studies. LDF and AB performed cation flux studies, phosphotyrosine analysis and contributed to the manuscript's preparation; AP carried out the mass spectrometric analysis.

The authors reported no potential conflicts of interest.

References

1. Stewart GW. Hemolytic disease due to membrane ion channel disorders. Curr Opin Hematol 2004;11:244-50.
2. Glader BE, Fortier N, Albala MM, Nathan DG. Congenital hemolytic anemia associated with dehydrated erythrocytes and increased potassium loss. N Engl J Med 1974;291:491-6.
3. Bruce LJ. Red cell membrane transport abnormalities. Curr Opin Hematol 2008;15:184-90.
4. Platt OS, Lux SE, Nathan DG. Exercise-induced hemolysis in xerocytosis. Erythrocyte dehydration and shear sensitivity. J Clin Invest 1981; 68:631-8.
5. Carella M, Stewart G, Ajetunmobi JF, Perrotta S, Grootenboer S, Tchernia G, et al. Genomewide search for dehydrated hereditary stomatocytosis (hereditary xerocytosis): mapping of locus to chromosome 16 (16q23-qter). Am J Hum Genet 1998; 63:810-6.
6. Carella M, d'Adamo AP, Grootenboer-Mignot S, Vantyghem MC, Esposito L, D'Eustacchio A, et al. A second locus mapping to 2q35-36 for familial pseudohyperkalaemia. Eur J Hum Genet 2004;12:1073-6.
7. Bruce LJ, Robinson HC, Guizouarn H, Borgese F, Harrison P, King MJ, et al. Monovalent cation leaks in human red cells caused by single amino-acid substitutions in the transport domain of the band 3 chloride-bicarbonate exchanger, AE1. Nat Genet 2005;37:1258-63.
8. Guizouarn H, Martial S, Gabillat N, Borgese F. Point mutations involved in red cell stomatocytosis convert the electroneutral anion exchanger 1 to a nonselective cation conductance. Blood 2007;110:2158-65.
9. Dodge JT, Mitchell C, Hanahan DJ. The preparation and chemical characteristics of hemoglobin-free ghosts of human erythrocytes. Arch Biochem Biophys 1963;100:119-30.
10. De Franceschi L, Rivera A, Fleming MD, Honczarenko M, Peters LL, Gascard P, et al. Evidence for a protective role of the Gardos channel against hemolysis in murine spherocytosis. Blood 2005;106:1454-9.
11. Biondani A, Turrini F, Carta F, Matte A, Filippini A, Siciliano A, et al. Heat-shock protein 27, -70 and peroxiredoxin II show molecular chaperone function in sickle red cells: evidence from transgenic sickle cell mouse model. Proteomics - Clinical Application 2008;706-19.
12. Brugnara C, Kopin AS, Bunn HF, Tosteson DC. Regulation of cation content and cell volume in hemoglobin erythrocytes from patients with homozygous hemoglobin C disease. J Clin Invest 1985;75:1608-17.
13. De Franceschi L, Olivieri O, Miraglia del Giudice E, Perrotta S, Sabato V, Corrocher R, et al. Membrane cation and anion transport activities in erythrocytes of hereditary spherocytosis: effects of different membrane protein defects. Am J Hematol 1997; 55:121-8.
14. De Franceschi L, Olivieri O, Girelli D, Lupo A, Bernich P, Corrocher R. Red blood cell cation transports in uraemic anaemia: evidence for an increased K/Cl co-transport activity. Effects of dialysis and erythropoietin treatment. Eur J Clin Invest 1995;25: 762-8.
15. Joiner CH, Rettig RK, Jiang M, Risinger M, Franco RS. Urea stimulation of KCl cotransport induces abnormal volume reduction in sickle reticulocytes. Blood 2007;109:1728-35.
16. De Franceschi L, Fumagalli L, Olivieri O, Corrocher R, Lowell CA, Berton G. Deficiency of Src family kinases Fgr and Hck results in activation of erythrocyte K/Cl cotransport. J Clin Invest 1997;99:220-7.
17. De Franceschi L, Biondani A, Carta F, Turrini F, Laudanna C, Deana R, et al. PTPepsilon has a critical role in signaling transduction pathways and phosphoprotein network topology in red cells. Proteomics 2008; 8:4695-708.
18. Roncada P, Cretich M, Fortin R, Agosti S, De Franceschi L, Greppi GF, et al. Acrylamide-agarose copolymers: improved resolution of high molecular mass proteins in two-dimensional gel electrophoresis. Proteomics 2005;5:2331-9.
19. Knauf PA, Pal P. Band 3 mediated transport. In Red Cell Membrane Transport in Health and Disease. Bernhardt I and Ellory JC, Editors. Springer, Berlin, 2003. p. 253-301.
20. Coles SE, Ho MM, Chetty MC, Nicolaou A, Stewart GW. A variant of hereditary stomatocytosis with marked pseudohyperkalaemia. Br J Haematol 1999;104:275-83.
21. Walsh MF, Ampasala DR, Hatfield J, Vander Heide R, Suer S, Rishi AK, et al. Transforming growth factor-beta stimulates intestinal epithelial focal adhesion kinase synthesis via Smad- and p38-dependent mechanisms. Am J Pathol 2008;173:385-99.
22. Perlman DF, Musch MW, Goldstein L. Cell membrane surface expression and tyrosine kinase regulate the osmolyte channel (skAE1) in skate erythrocytes. Acta Physiol 2006; 187:87-91.
23. Tilly BC, van den Berghe N, Tertoolen LG, Edixhoven MJ, de Jonge HR. Protein tyrosine phosphorylation is involved in osmoregulation of ionic conductances. J Biol Chem 1993;268:19919-22.
24. Varela D, Simon F, Riveros A, Jorgensen F, Stutzin A. NAD(P)H oxidase-derived H(2)O(2) signals chloride channel activation in cell volume regulation and cell proliferation. J Biol Chem 2004;279:13301-4.
25. Olivieri O, Girelli D, Vettore L, Balercia G, Corrocher R. A case of congenital dyserythropoietic anaemia with stomatocytosis, reduced bands 7 and 8 and normal cation content. Br J Haematol 1992; 80:258-60.
26. Jarvis HG, Chetty MC, Nicolaou A, Fisher J, Miller A, Stewart GW. A novel stomatocytosis variant showing marked abnormalities in intracellular [Na] and [K] with minimal haemolysis. Eur J Haematol 2001; 66:412-4.
27. Paw BH, Davidson AJ, Zhou Y, Li R, Pratt SJ, Lee C, et al. Cell-specific mitotic defect and dyserythropoiesis associated with erythroid band 3 deficiency. Nat Genet 2003;34:59-64.
28. Mentzer WC Jr, Smith WB, Goldstone J, Shohet SB. Hereditary stomatocytosis: membrane and metabolism studies. Blood 1975;46: 659-69.
29. Rivera A, De Franceschi L, Peters LL, Gascard P, Mohandas N, Brugnara C. Effect of complete protein 4.1R deficiency on ion transport properties of murine erythrocytes. Am J Physiol Cell Physiol 2006;291:C880-6.
30. Bordin L, Ion-Popa F, Brunati AM, Clari G, Low PS. Effector-induced Syk-mediated phosphorylation in human erythrocytes. Biochim Biophys Acta 2005;1745:20-8.
31. Harrison ML, Isaacson CC, Burg DL, Geahlen RL, Low PS. Phosphorylation of human erythrocyte band 3 by endogenous p72syk. J Biol Chem 1994;269:955-9.
32. Brunati AM, Bordin L, Clari G, James P, Quadroni M, Baritono E, et al. Sequential phosphorylation of protein band 3 by Syk and Lyn tyrosine kinases in intact human erythrocytes: identification of primary and secondary phosphorylation sites. Blood 2000;96:1550-7.
33. Anong WA, Weis TL, Low PS. Rate of rupture and reattachment of the band 3-ankyrin bridge on the human erythrocyte membrane. J Biol Chem 2006;281:22360-6.
34. Li J, Dao M, Lim CT, Suresh S. Spectrin-level modeling of the cytoskeleton and optical tweezers stretching of the erythrocyte. Biophys J 2005;88:3707-19.
35. Musch MW, Hubert EM, Goldstein L. Volume expansion stimulates p72(syk) and p56(lyn) in skate erythrocytes. J Biol Chem 1999;274: 7923-8.
36. Musch MW, Goldstein L. Tyrosine kinase inhibition affects skate anion exchanger isoform I alterations after volume expansion. Am J Physiol Regul Integr Comp Physiol 2005; 288:R885-90.
37. Salzer U, Hinterdorfer P, Hunger U, Borken C, Prohaska R. Ca(++)-dependent vesicle release from erythrocytes involves stomatin-specific lipid rafts, synexin (annexin VII), and sorcin. Blood 2002;99:2569-77.
38. Salzer U, Ahorn H, Prohaska R. Identification of the phosphorylation site on human erythrocyte band 7 integral membrane protein: implications for a monotopic protein structure. Biochim Biophys Acta 1993; 1151:149-52.
39. Miraglia del Giudice E, Iolascon A, Pinto L, Nobili B, Perrotta S. Erythrocyte membrane protein alterations underlying clinical heterogeneity in hereditary spherocytosis. Br J Haematol 1994;88:52-5.